Cyclic Variation and Solar Forcing of Holocene Climate in the Alaskan Subarctic

Feng Sheng Hu,[1,2,3]* Darrell Kaufman,[4] Sumiko Yoneji,[1] David Nelson,[2] Aldo Shemesh,[5] Yongsong Huang,[6] Jian Tian,[3] Gerard Bond,[7] Benjamin Clegg,[1] Thomas Brown[8]

High-resolution analyses of lake sediment from southwestern Alaska reveal cyclic variations in climate and ecosystems during the Holocene. These variations occurred with periodicities similar to those of solar activity and appear to be coherent with time series of the cosmogenic nuclides ^{14}C and [10]Be as well as North Atlantic drift ice. Our results imply that small variations in solar irradiance induced pronounced cyclic changes in northern high-latitude environments. They also provide evidence that centennial-scale shifts in the Holocene climate were similar between the subpolar regions of the North Atlantic and North Pacific, possibly because of Sun-ocean-climate linkages.

Small variations in solar output appear to have played a prominent role in the Holocene dynamics of the earth's climate system. Although the mechanisms for Sun-climate linkages at sub-Milankovitch time scales remain a focus of debate (*1*, *2*), evidence is emerging in proxy records (*3–7*). Such linkages have profound implications for the dynamics of the earth's climate system, but they are untested in some key regions. In the subpolar North Pacific, numerous continental records of Holocene climatic change exist (*8–10*). However, they all lack the temporal resolution adequate to detect solar-induced climatic variations at centennial time scales, making it difficult to assess the potential climatic connection between the North Pacific and other regions.

Here we report the results of biological and geochemical analyses (*11*) of sediment from a tundra lake in southwestern Alaska. Arolik Lake (59°28′N, 161°07′W, 145 m above sea level) (Fig. 1) is in a moraine-dammed basin located along the southwestern flank of the Ahklun Mountains. Its sediment bed was surveyed acoustically to yield results that guided the selection of core sites and allowed the correlation of stratigraphic units (*12*). Four cores were recovered with a percussion corer; the unconsolidated sediment of the last ~2300 years was lost in core retrieval. We focus here on the Holocene section of core AL-4 (circa 12 to 2.3 thousand years ago), the chronology of which is based on nine calibrated accelerator mass spectrometry radiocarbon dates on terrestrial plant macrofossils, plus the age of a well-known tephra layer (Fig. 2A and table S1). The section was analyzed at contiguous 1-cm intervals (equivalent to 45 years on average) for its contents of biogenic silica (BSi), organic carbon (OC), and organic nitrogen (ON). Selected samples were analyzed for pollen assemblages, oxygen-isotopic composition of diatom silica ($\delta^{18}O_{Si}$), and hydrogen-isotopic composition of palmitic acid (δD_{PA}) to provide additional constraints on environmental interpretation.

Large fluctuations occur in various proxy indicators in the Arolik Lake record (Fig. 2A). We describe the BSi profile in detail because of its high temporal resolution plus its relatively unambiguous environmental signals. BSi reflects the sedimentary abundance of diatoms, which are single-celled algae that commonly dominate lake primary productivity (*13*). BSi fluctuates between ~80 and ~340 mg/g from 12,000 to 2300 years ago (Fig. 2A), suggesting pronounced changes in aquatic productivity. During the last glacial-interglacial transition (LGIT), BSi exhibits patterns resembling those of the Younger Dryas (YD) oscillation seen in the Greenland Ice Sheet Project 2 (GISP2) $\delta^{18}O$ record (Fig. 2A) (*14*), as at other sites in southwestern Alaska (*9*, *15*). The interpretation that BSi reflects aquatic productivity is supported by the positive correlations of BSi with sedimentary OC and ON, which also derive mainly from aquatic production as inferred from the low OC:ON ratios of 7 to 12 throughout the record (*16*). BSi and the OC:ON ratio are negatively correlated, although the correlation is weaker than those of BSi versus OC and BSi versus ON. This relationship provides additional support that diatom productivity, instead of other factors such as dilution by detrital minerals, drives variations in BSi, OC, and ON. Furthermore, stratigraphic changes in the cell net abundance of the algal group *Pediastrum* [similar to those of principal component analysis (PCA) axis 1 discussed below] in the same core mimic the stratigraphic changes in BSi.

In addition to aquatic changes, palynological analysis shows that terrestrial vegetation experienced pronounced synchronous fluctuations. We used PCA to summarize our pollen percentage results. The first principal component (PCA axis 1) accounts for 34.2% of the variance, and its stratigraphic variation is similar to that of BSi (correlation coefficient $r = 0.76$, $P < 0.0001$) (Fig. 2B). This axis is driven primarily by the shrub taxon *Betula* and *Pediastrum*, which have the highest scores, and by the herbaceous and fern taxa *Arte-*
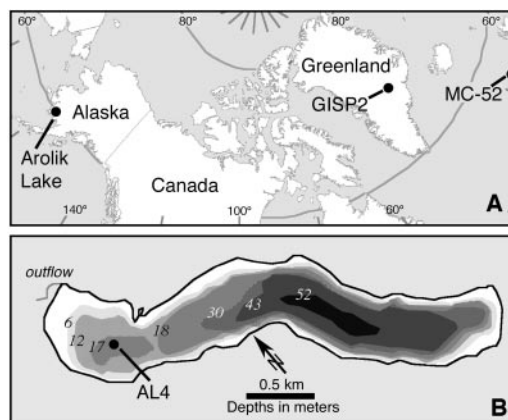
[1]Department of Plant Biology, [2]Program in Ecology and Evolutionary Biology, [3]Department of Geology, University of Illinois, Urbana, IL 61801, USA. [4]Departments of Geology and Environmental Sciences, Northern Arizona University, Flagstaff, AZ 86011, USA. [5]Department of Environmental Sciences, The Weizmann Institute of Science, Rehovot 76100, Israel. [6]Department of Geological Sciences, Brown University, Providence, RI 02912, USA. [7]Lamont-Doherty Earth Observatory of Columbia University, Palisades, NY 10964, USA. [8]Center for Accelerator Mass Spectrometry–Lawrence Livermore National Laboratory, Livermore, CA 94551, USA.

*To whom correspondence should be addressed. E-mail: fshu@life.uiuc.edu

Fig. 1. (A) Map showing locations of Arolik Lake and other sites discussed in the text. MC-52, sediment core MC52-VM29-191 (*3*). (B) Bathymetry of Arolik Lake and the core site.

misia and *Polypodiaceae*, which have the lowest scores. The pollen abundance of *Betula*, a dominant shrub type at this tundra site, fluctuates by up to 25% between adjacent BSi troughs and peaks, suggesting pronounced changes in shrub density (*17, 18*) in accordance with those of aquatic productivity. The abundance of *Betula* shrubs is positively related to temperature and moisture in the Alaskan tundra (*18–20*), likely with temperature being more important in coastal southwestern Alaska. We interpret higher PCA axis 1 scores as indicating warmer and wetter conditions.

Analyses of $\delta^{18}O_{Si}$ and δD_{PA} on the same core (Fig. 2B) further elucidate climatic changes. These isotopic proxies have been successfully applied in paleoclimatic studies at other lakes where sedimentary carbonate is absent (*15, 21–23*). $\delta^{18}O_{Si}$ and δD_{PA} are positively related to lake-water oxygen and hydrogen isotopic compositions, respectively, ($\delta^{18}O$), which in turn are determined by a number of other fac-

tors, such as air temperature, moisture source, and evaporation. $\delta^{18}O_{Si}$ is also a negative function of water temperature (*24*), whereas the hydrogen-isotopic fractionation of palmitic acid does not vary with water temperature (*21, 25*). The fact that both $\delta^{18}O_{Si}$ and δD_{PA} are negatively correlated with BSi suggests that water temperature was not the primary driver of isotopic fractionation and ecosystem changes. Atmospheric temperature changes alone cannot account for the relationships among $\delta^{18}O_{Si}$, δD_{PA}, BSi, and pollen PCA axis 1, because it is very unlikely that atmospheric cooling, which would be registered as decreases in both $\delta^{18}O_{Si}$ and δD_{PA} (*15, 21*), could have increased aquatic productivity and *Betula* shrub abundance at this site.

Instead, the patterns in all of the proxy indicators described above can be best reconciled by variations in both effective moisture (precipitation minus evaporation) and atmospheric temperature. An increase in effective

moisture, especially one due to increased snowfall, would have caused decreased $\delta^{18}O_{Si}$ and δD_{PA} at Arolik Lake, which today is a nearly closed basin sensitive to water-balance fluctuations. This effect probably masked the isotopic signals of increased temperature. Increases in temperature and moisture would have favored the expansion of *Betula* shrubs and enhanced nutrient input to the lake from the watershed (*19, 20, 26, 27*), thereby stimulating diatom productivity and increasing sedimentary BSi content.

The magnitudes of Holocene climatic change, as inferred from BSi at Arolik Lake, are as large as those of the YD oscillation (Fig. 2A). This pattern stands in sharp contrast with paleoclimate records from the circum-North Atlantic, such as GISP2 $\delta^{18}O$ (*14*) (Fig. 2A), which shows that climatic variability is much smaller during the Holocene than during the LGIT. Two factors may account for this discrepancy. First, the magnitudes of the YD climatic fluctuations were relatively small in the North Pacific region compared with those of the North Atlantic (*15, 28*). Second, lake productivity probably responded nonlinearly to climatic change, with amplifying effects during the Holocene. For example, the amount of nutrients (e.g., nitrogen and phosphorus) released from decomposition was probably greater during the Holocene, when organic soils were thicker and the active layer deeper than during the Late Glacial.

Spectral analyses (*11*) of the Holocene BSi record from Arolik Lake show periodicities of 135, 170, 195, 435, 590, and 950 years above the 90% confidence level (Fig. 3), suggesting cyclic climatic changes at centennial scales. Within the limits of our ^{14}C chronology, several of these periodicities coincide with known solar cycles. For example, the 195-year period is similar to the well-known de Vries solar cycle of ~200 years, and periodicities of 400 to 500 and ~950 years have been documented in residual atmospheric ^{14}C production ($\Delta^{14}C$) data (*29*) and a proxy record of the North Atlantic Deep Water (NADW) (*30*). Although long-term $\Delta^{14}C$ patterns may have been affected by climatic change and the carbon cycle, recent studies (*31, 32*) comparing ^{10}Be and $\Delta^{14}C$ records have made a strong case that Holocene $\Delta^{14}C$ variation reflects dominantly solar modulation. Thus, the spectral similarity implies that solar variation was an important trigger of Holocene cyclic environmental changes in Alaska.

Corroborating this inference is the coherency between our BSi record and the time series of atmospheric ^{10}Be and ^{14}C productions (Fig. 2C) (*3, 33–35*). The production rates of these two cosmogenic nuclides are negatively related to the strength of magnetic
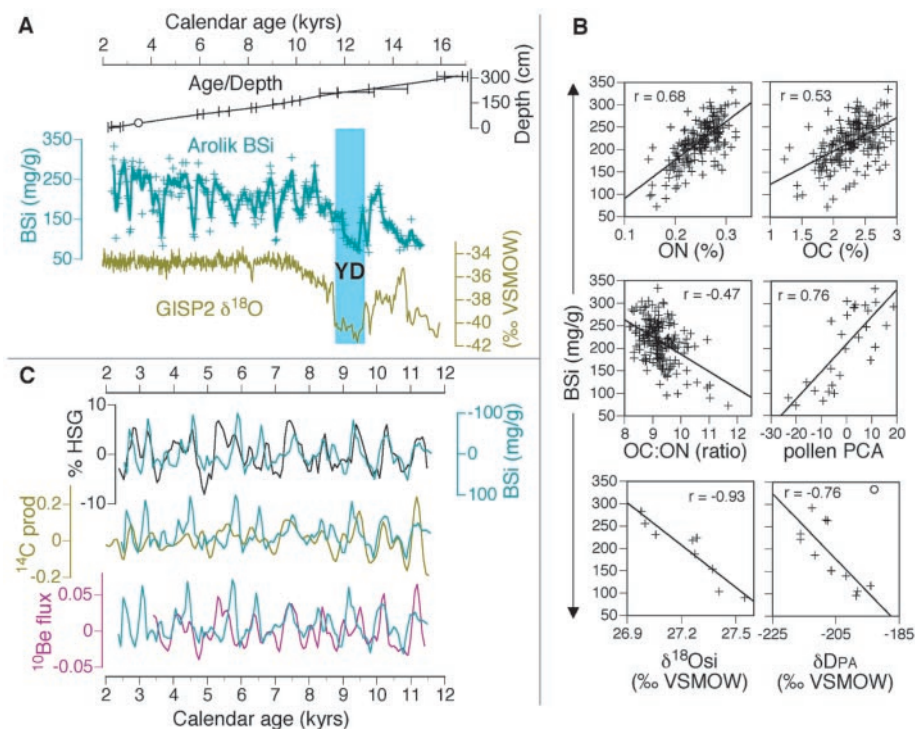

Fig. 2. Proxy records of climatic change and solar activity. (**A**) Age-depth model and comparisons of the Arolik Lake BSi (expressed in mg per g of dry sediment) record with ice-core $\delta^{18}O$ data from GISP2. For the age-depth curve, error bars are 2σ ranges; the open circle represents the Aniakchak tephra age (*11*). In the BSi plot, crosses represent raw data, and the curve shows 5-point running averages. kyrs, thousand years; VSMOW, Vienna standard mean ocean water. (**B**) The relationships of BSi with other climatic and ecological proxies. Pollen PCA data are the PCA Axis 1 scores of the percentages of major pollen types. *Alnus* and *Picea* were excluded in the pollen sum for percentage calculations, because these two types first appeared in the middle and late Holocene, respectively, and because *Picea* was not locally present in the Arolik Lake area. The open circle in the BSi-δD_{PA} plot is an outlier that was excluded in the correlation analysis. (**C**) Comparisons of the Arolik Lake BSi record (teal curve in all three plots) with % HSG, ^{14}C production rate (^{14}C prod, in atoms cm^{-2} s^{-1}), and ^{10}Be flux (in 10^5 atoms cm^{-2} year^{-1}) from (*3*). All data were detrended and smoothed with the same procedures as in (*3*). BSi scales are reversed. The ^{14}C chronology of % HSG was shifted by ~200 years throughout the record; no chronological shifts were made for any other time series.

fields embedded in solar winds and to solar wind speed. Reduced magnetic fields and weaker solar winds appear to be related to reduced total solar irradiance, although the exact relation among these parameters is unclear (*36*, *37*). Furthermore, the BSi record exhibits patterns opposite to variations of hematite-stained-grain abundance (% HSG) in core MC52-VM29-191, the best-dated proxy record of drift ice from the North Atlantic, which has been shown to correlate with both [10]Be and ^{14}C records (*3*). Thus, increases in temperature and moisture at Arolik Lake apparently corresponded to intervals of elevated solar output and reduced advections of ice-bearing (cooler) surface waters eastward and southward in the North Atlantic. Conversely, decreases in temperature and moisture corresponded to intervals of reduced solar output and increased advections of North Atlantic ice-bearing waters.

The peaks and troughs of BSi, [10]Be flux, ^{14}C production, and % HSG are markedly consistent, given the inherent limitations of ^{14}C chronologies for the BSi and % HSG records. However, substantial discrepancies do exist when any two of these records are compared in detail. For example, the correlation is poor between 6000 and 5000 years ago; the % HSG profile exhibits a broad peak that is much narrower in the BSi record and less prominent in the ^{14}C and [10]Be data. In addition, the BSi and % HSG records are offset by ~200 years, with the latter leading the former. The reasons for these discrepancies are unclear, although this 200-year offset is well within the 2σ ranges of the calibrated ^{14}C dates [see supporting online material in (*3*)]. Alternatively, this offset may come from ^{14}C reservoir corrections in the North Atlantic or reflect the time for the transmission of an ocean signal from the North Atlantic to the North Pacific. We also note that our spectral analysis reveals a peak of ~1500 years, a quasi-periodic pacing of North Atlantic drift-ice abundance (*3*, *38*), that is above the 80% confidence level but not above the 90% level.

The general correspondence of prominent environmental changes in southwestern Alas-

ka to variations in solar energy output and North Atlantic drift ice implies a solar influence on hemispheric-scale climatic oscillations during the Holocene. Such Sun-climate relationships are plausible on the basis of recent atmospheric general circulation modeling. For example, a 0.1% decrease in solar irradiance related to the 11-year sunspot cycle could alter the atmosphere's dynamic response to changes in stratospheric ozone and temperature, producing a change in surface climate (*39*, *40*). On multidecadal scales, Shindell et al. (*41*) demonstrated that an estimated ~0.25% reduction of solar irradiance during the Maunder Minimum resulted in surface climatic patterns over the Northern Hemisphere similar to those associated with the low index state of the Arctic Oscillation (AO)/North Atlantic Oscillation (NAO). Their simulations showed that reduced solar output led to diminished moisture over Alaska and decreased sea-surface temperatures over portions of the North Atlantic. This spatial pattern is broadly consistent with our proxy record and those of Bond et al. (*3*), supporting the hypothesis that solar variations can have hemispheric-scale climatic consequences by altering the AO/NAO (*41*).
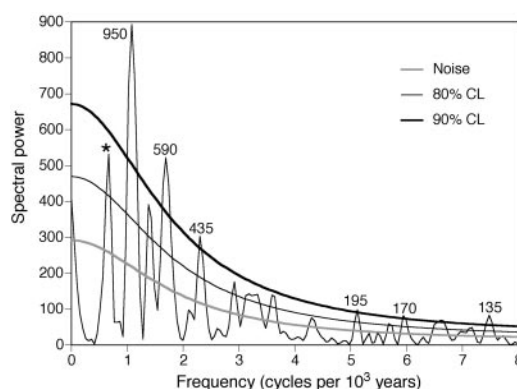
However, within the circum–North Atlantic, climate records at multicentennial to millennial scales appear to be discordant with the distinct AO/NAO dipole anomaly, implicating NADW as a dominant climatic control at least within that region (*3*). Bond et al. (*3*) suggest that, through its effects on sea ice, solar variation affects NADW formation, thereby amplifying the effects of small variations in solar irradiance on the earth's climate over the Holocene. According to model simulations that include an active ocean (*42*), decreases in NADW production would have the same effect on atmospheric water vapor flux in the North Pacific as expected from a reduced AO/NAO. Hence, with the evidence presently available, it is impossible to distinguish whether a shift in the AO/NAO or NADW, or the combined effect of the two in a coupled ocean-atmosphere system, was the dominant influence.

Our data offer support for the notion that Holocene climatic change occurred in a cyclic fashion at frequencies longer than those detectable by instrumental records. Cyclicity implies predictability; thus, if such climatic cycles indeed exist, they would add an important dimension to improve predictions of future changes. Equally important, our results illustrate that subtle solar variations can lead to pronounced changes in high-latitude terrestrial and freshwater ecosystems, which may in turn exert important feedback to climatic change (*26*, *27*). Furthermore, our data suggest that centennial-scale shifts in the Holocene climate were similar between the subpolar regions of the North Atlantic and North Pacific, possibly because of Sun-ocean-climate linkages. Documenting such connection between these two key regions of the earth's system is an important step toward understanding mechanisms of global climatic change.

References and Notes

1. D. Rind, *Science* **296**, 673 (2002).
2. K. S. Carslaw, R. G. Harrison, J. Kirkby, *Science* **298**, 1732 (2002).
3. G. Bond et al., *Science* **294**, 2130 (2001).
4. D. Fleitmann et al., *Science* **300**, 1737 (2003).
5. A. K. Gupta, D. M. Anderson, J. T. Overpeck, *Nature* **421**, 354 (2003).
6. D. A. Hodell, M. Brenner, J. H. Curtis, T. Guilderson, *Science* **292**, 1367 (2001).
7. D. Verschuren, K. R. Laird, B. F. Cumming, *Nature* **403**, 410 (2000).
8. P. M. Anderson, L. B. Brubaker, *Quat. Sci. Rev.* **13**, 71 (1994).
9. L. B. Brubaker, P. M. Anderson, F. S. Hu, *Quat. Sci. Rev.* **20**, 175 (2001).
10. A. V. Lozhkin et al., *Quat. Res.* **39**, 314 (1993).
11. Materials and methods are available as supporting material on *Science* Online.
12. D. S. Kaufman et al., *J. Paleolimnol.*, in press.
13. R. G. Wetzel, *Limnology: Lake and River Ecosystems* (Academic Press, San Diego, CA, ed. 3, 2001).
14. M. Stuiver, P. M. Grootes, T. F. Braziunas, *Quat. Res.* **44**, 341 (1995).
15. F. S. Hu, A. Shemesh, *Quat. Res.* **59**, 379 (2003).
16. P. A. Meyers, E. Lallier-Verges, *J. Paleolimnol.* **21**, 345 (1999).
17. P. M. Anderson, P. J. Bartlein, L. B. Brubaker, K. Gajewski, J. C. Ritchie, *J. Biogeogr.* **18**, 565 (1991).
18. W. W. Oswald, P. M. Anderson, L. B. Brubaker, F. S. Hu, D. R. Engstrom, *J. Biogeogr.* **30**, 521 (2003).
19. F. S. Chapin, G. R. Shaver, A. E. Giblin, K. J. Nadelhoffer, J. A. Laundre, *Ecology* **76**, 694 (1995).
20. M. Sturm, C. Racine, K. Tape, *Nature* **411**, 546 (2001).
21. Y. S. Huang, B. Shuman, Y. Wang, T. Webb, *Geology* **30**, 1103 (2002).
22. P. A. Barker et al., *Science* **292**, 2307 (2001).
23. M. Rietti-Shati, A. Shemesh, W. Karlen, *Science* **281**, 980 (1998).
24. A. Shemesh, C. D. Charles, R. G. Fairbanks, *Science* **256**, 1434 (1992).
25. M. F. Estep, T. C. Hoering, *Geochim. Cosmochim. Acta* **44**, 1197 (1980).
26. G. E. Liston, J. P. McFadden, M. Sturm, R. A. Pielke, *Global Change Biol.* **8**, 17 (2002).
27. M. Sturm et al., *J. Clim.* **14**, 336 (2001).
28. U. Mikolajewicz, T. J. Crowley, A. Schiller, R. Voss, *Nature* **387**, 384 (1997).
29. M. Stuiver, T. F. Braziunas, *Radiocarbon* **35**, 137 (1993).
30. M. R. Chapman, N. J. Shackleton, *Holocene* **10**, 287 (2000).
31. R. Muscheler, J. Beer, G. Wagner, R. C. Finkel, *Nature* **408**, 567 (2000).
32. J. Beer et al., *Nature* **331**, 675 (1988).

Fig. 3. Spectral patterns of the Holocene BSi record from Arolik Lake. Numbers within the graph are spectral peaks in years above the 90% confidence level (CL) based on a χ^2 test. The asterisk indicates a 1500-year periodicity above the 80% CL.

33. R. C. Finkel, K. Nishiizumi, *J. Geophys. Res.* **102 (C12)**, 26699 (1997).
34. M. Stuiver *et al.*, *Radiocarbon* **40**, 1041 (1998).
35. F. Yiou *et al.*, *J. Geophys. Res.* **102**, 26783 (1997).
36. P. Foukal, *Geophys. Res. Lett.* **29**, 2089 (2002).
37. J. L. Lean, Y. M. Wang, N. R. Sheeley, *Geophys. Res. Lett.* **29**, 2224 (2002).
38. G. Bond *et al.*, *Science* **278**, 1257 (1997).
39. J. D. Haigh, *Science* **272**, 981 (1996).
40. D. T. Shindell, D. Rind, N. Balachandran, J. Lean, P. Lonergan, *Science* **284**, 305 (1999).
41. D. T. Shindell, G. A. Schmidt, M. E. Mann, D. Rind, A. Waple, *Science* **294**, 2149 (2001).
42. A. Schiller, U. Mikolajewicz, R. Voss, *Clim. Dyn.* **13**, 325 (1997).
43. We thank D. Shindell, H. Wright, T. Johnson, D. Peteet, and two anonymous reviewers for comments; Y. Axford, J. Briner, and A. Werner for field assistance; and J. Bright and S. McMillan for laboratory assistance. Supported by a Packard Fellowship in Science and Engineering (F.S.H.); NSF grant nos. ATM-9996064 and ATM-0318404 (F.S.H.), EAR-9808593 (D.K.), and ATM-0081478 (Y.S.H.); and an Israeli Science Foundation grant (A.S.). Radiocarbon dating was performed, in part, under the auspices of the U.S. Department of Energy by the University of California, Lawrence Livermore National Laboratory under contract no. W-7405-Eng-48. NSF Paleoenvironmental Arctic Sciences (PARCS) contribution number 212.

Intensive Pre-Incan Metallurgy Recorded by Lake Sediments from the Bolivian Andes

Mark B. Abbott[1]*† and Alexander P. Wolfe[2]†

The history of pre-Columbian metallurgy in South America is incomplete because looting of metal artifacts has been pervasive. Here, we reconstruct a millennium of metallurgical activity in southern Bolivia using the stratigraphy of metals associated with smelting (Pb, Sb, Bi, Ag, Sn) from lake sediments deposited near the major silver deposit of Cerro Rico de Potosí. Pronounced metal enrichment events coincide with the terminal stages of Tiwanaku culture (1000 to 1200 A.D.) and Inca through early Colonial times (1400 to 1650 A.D.). The earliest of these events suggests that Cerro Rico ores were actively smelted at a large scale in the Late Intermediate Period, providing evidence for a major pre-Incan silver industry.

New World metallurgy emerged in the Andean region of South America between the Initial Period (1800 to 900 B.C.) and the Early Horizon (900 to 200 B.C.) (*1*). The oldest well-dated archaeological site containing metal artifacts is Mina Perdida (Lurín Valley) in coastal Peru, where hammered foils and gilded copper are preserved in contexts dating to 1400 to 1100 B.C. (*2*). The tradition of sheet-metal working (hammering, gilding, annealing, and *repoussé*) remained pervasive in the Andes throughout the Early Intermediate Period (200 B.C. to 600 A.D.) and the Middle Horizon (600 to 1100 A.D.) (*3*). By 1000 A.D., large-scale copper smelting and bronze production is evident at sites such as Batán Grande on the northern Peruvian coast (*4*). Beginning in the Late Intermediate Period (1100 to 1450 A.D.), intensive copper working became widespread on the Bolivian *altiplano*, with the production of materials of copper-tin alloy (i.e., bronze), in contrast to the copper-arsenic artifacts found in Peru (*5*). By this time, silver and gold were well-established as precious metals among Andean cultures. Although silver was highly sought by royalty for symbolic and ritual purposes (*6*), the geographic distribution, intensity, and timing of Late Intermediate Period silver mining in the Andes remains unclear. Here, we infer a regional history of metallurgy from lake sediments retrieved adjacent to the largest silver deposit of the Bolivian tin belt.

Laguna Lobato (hereafter LL) (*7*) is small (0.2 km²), relatively deep (11 m), and occupies a nonglacial catchment of 3.9 km² (Fig. 1). The lake overflows only during the wet season (December to March), and it has no hydrological connection with surface waters draining Cerro Rico, 6 km west of the lake. Because westerly winds prevail for 8 months of the year (April to November) (*8*), LL is strategically located to record atmospheric deposition of metals volatilized during smelting or transported as fine-grain particulates. This study is based on a 74.5-cm core recovered from the deepest portion of the lake and dated by ^{210}Pb, ^{137}Cs, (table S1), and ^{14}C analyses (*9*) (table S2).

Cerro Rico lies within a zone of xenothermal mineralization related to Middle Tertiary intrusions (*10*). In addition to native silver, the richest ores contain combinations of acanthite (Ag_2S), andorite ($PbAgSb_3S_6$), chlorargyrite ($AgCl$), matildite ($AgBiS_2$), miargyrite ($AgSbS_2$), pyrargyrite (Ag_3SbS_3), and tetrahedrite [$(Ag, Cu, Fe, Zn)_{12}Sb_4S_{13}$] (*11*). Tin is associated primarily with cassiterite (SnO_2). To assess the history of smelting, we measured the concentrations in lake sediments of five metals (Ag, Bi, Pb, Sb, and Sn) associated with ore composition (*9*). Of these metals, Pb serves as the cornerstone of our interpretations for two reasons. First, the Incan smelting technology relied on argentiferous galena [*soroche* (Pb, Ag)S] as a flux during smelting, which was conducted in charcoal-fired, wind-drafted furnaces lined with clay (*huayras*) (*12, 13*). The use of *soroche* led to excessive Pb volatilization, resulting in lake sediment concentrations that are orders of magnitude higher than those of the other analyzed metals. Second, Pb is largely immobile once deposited in lake sediments (*14, 15*). Although molecular diffusion rates for Ag are higher than those for Pb (*16, 17*), in both cases they are insignificant in comparison to average sediment accumulation rates in LL (~1 mm year^{-1}). Thus, postdepositional mobility is not a confounding factor in the interpretation of the record, a conclusion supported by the largely parallel trends observed for each of the metals.

Before 1000 A.D., concentrations of all five metals in the sediments of LL were low and stable, representing natural background levels of metal accumulation (Fig. 2). An additional 15 samples spanning the earlier period from 2000 B.C. to 600 A.D. have similarly low Pb
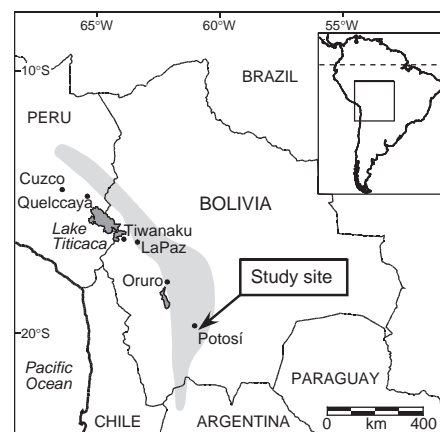

Fig. 1. Location map of the study site in relation to the Tiwanaku capital, Lake Titicaca, Potosí, and the Quelccaya ice core. The shaded area indicates the central Bolivian tin belt (*27*), which broadly corresponds to the crest of the Andean cordillera.

[1]Department of Geology and Planetary Science, University of Pittsburgh, Pittsburgh, PA 15260, USA. [2]Department of Earth and Atmospheric Sciences, University of Alberta, Edmonton, AB T6G 2E3, Canada.

*To whom correspondence should be addressed. E-mail: mabbott1@pitt.edu
†Both authors contributed equally to this work.